

Stabilizer configuration interaction: Finding molecular subspaces with error detection properties

Abhinav Anand^{1,2,*} and Kenneth R. Brown^{1,2,3,4,†}

¹*Duke Quantum Center, Duke University, Durham, NC 27701, USA.*

²*Department of Electrical and Computer Engineering, Duke University, Durham, NC 27708, USA.*

³*Department of Physics, Duke University, Durham, NC 27708, USA.*

⁴*Department of Chemistry, Duke University, Durham, NC 27708, USA.*

(Dated: October 29, 2024)

In this work, we explore a new approach to designing both algorithms and error detection codes for preparing approximate ground states of molecules. We propose a classical algorithm to find the optimal stabilizer state by using excitations of the Hartree-Fock state, followed by constructing quantum error-detection codes based on this stabilizer state using codeword-stabilized codes. Through various numerical experiments, we confirm that our method finds the best stabilizer approximations to the true ground states of molecules up to 36 qubits in size. Additionally, we construct generalized stabilizer states that offer a better approximation to the true ground states. Furthermore, for a simple noise model, we demonstrate that both the stabilizer and (some) generalized stabilizer states can be prepared with higher fidelity using the error-detection codes we construct. Our work represents a promising step toward designing algorithms for early fault-tolerant quantum computation.

I. INTRODUCTION

In recent years, various demonstrations of fault-tolerant (FT) operations on physical devices [1–7] have been carried out, leading to proposals for their use in early fault-tolerant [8, 9] quantum computing. A common theme of these proposals is developing methods [10–15] that require low overhead (such as the number of logical qubits, operations, and T-count) for the fault-tolerant implementation of different algorithms. While this is an important and promising research direction, the overhead [16] associated with these proposals can still be prohibitively high.

A key reason for the extremely high overhead is the significant resources required for encoding information in logical qubits. To address this, we explore a new approach that designs both algorithms and error detection codes for preparing approximate ground states of molecules [17–19]. Our approach involves using the approximate eigenspace (spanned by a few stabilizer states) of the physical system we are simulating as the code space of the error detection codes.

Recent studies [20–24] have proposed various methods for constructing approximate eigenstates of different physical systems. However, most of these methods involve building parameterized quantum circuits [25–32] or Clifford circuits [33–37] and performing optimization [38–45] to find the best approximations. This makes these methods computationally expensive and limits their applicability to smaller systems as they have various limitations. [46–49] To overcome this limitation, we propose an efficient classical algorithm for construct-

ing stabilizer approximations of the ground states [50] of various molecules. We present results from various numerical experiments that approximate the ground state of various molecules of size up to 36 qubits. Our numerical experiments range from taking just seconds for smaller molecules like H_2 to several hours for larger ones like Cr_2 , which is a significant improvement over previous methods, where computations of this scale could take anywhere from minutes to weeks [36].

Subsequently, we construct quantum codes using codeword stabilized codes [51] based on the stabilizer approximations of the ground states. These codes are error detection codes with a single logical qubit and require minimal resources to prepare the states using error-detection and post-selection.

While the states we construct may not achieve the desired accuracy for most of the molecules considered in this study, our work represents a significant step towards the design of algorithms suitable for implementation on early fault-tolerant quantum computers.

The remainder of the paper is organized as follows: We begin with a review of preliminary theory and background information in Sec. II. The algorithm and results from various numerical experiments are discussed in Sec. III. In Sec. IV, we present the details of the codes and demonstrate the error-detection property of the method. Finally, we provide concluding remarks in Sec. V.

II. THEORY AND BACKGROUND

In this section, we review some of the essential theory and background information required for the rest of the paper.

* E-mail: abhinav.anand@duke.edu

† E-mail: kenneth.r.brown@duke.edu

A. Hartree-Fock and configuration interaction wavefunctions

In this article, we consider the second quantized formalism, where the state of a qubit represents the occupancy of a spin-orbital basis function.

The Hartree-Fock (HF) state [52, 53] in this formalism is a single product wavefunction with the minimal energy. One solves a set of self-consistent field (SCF) equations to determine the optimal molecular orbitals that minimize the total electronic energy of the system. Using the optimized molecular orbitals as a basis, the n -qubit Hartree-Fock state can be written as:

$$|\text{HF}\rangle = |\underbrace{11\dots 11}_{n_o} 00\dots 00\rangle, \quad (1)$$

where n_o is the number of occupied spin orbitals.

Using the HF state as a reference state, one can create a linear combination of configurations (excitations). The exact ground state solution is the full configuration interaction (FCI) wavefunction [52, 53] $|\text{FCI}\rangle$ and requires a sum over all possible excitations.

$$|\text{FCI}\rangle = \sum_k^{n_o} \hat{C}_k |\text{HF}\rangle, \quad (2)$$

$$\hat{C}_k = \sum_{i < j < \dots}^o \sum_{a < b < \dots}^{\text{vir}} c_{ij\dots}^{ab\dots} \hat{a}_i^\dagger \hat{a}_b^\dagger \dots \hat{a}_i \hat{a}_j \dots, \quad (3)$$

where $c_{ij\dots}^{ab\dots}$ denotes complex coefficients and \hat{C}_k is an operator consisting of k annihilation operators, \hat{a}_i , and k creation operators, \hat{a}_a^\dagger , acting on the occupied and virtual orbitals, respectively. The operator \hat{C}_k generates a k -fold configuration.

B. Stabilizer states

A stabilizer state [54] is defined as a n -qubit pure state $|\psi_s\rangle$, which is stabilized by an abelian subgroup \mathcal{S} of the Pauli group \mathcal{G}_n , i.e.,

$$P |\psi_s\rangle = |\psi_s\rangle; \forall P \in \mathcal{S}, \quad (4)$$

where P is a Pauli-string (tensor product of Pauli matrices I, X, Y and Z) on n -qubits.

The stabilizer group \mathcal{S} , is local-Clifford equivalent to a graph state [55, 56], so there exists a local Clifford unitary that maps every stabilizer to the form $X_v Z_{\{n\}}$, where v represents a vertex in the graph and $\{n\}$ is the corresponding set of neighbors.

It is well known [57] that given two n -qubit stabilizer states, $|\psi\rangle$ and $|\phi\rangle$, $\frac{|\psi\rangle + i^l |\phi\rangle}{\sqrt{2}}$ is also a stabilizer state, iff $\langle \phi | \psi \rangle = 0$ and $|\phi\rangle = P |\psi\rangle$, where $l \in \{0, 1, 2, 3\}$ and $P \in \mathcal{G}_n$.

C. Codeword stabilized (CWS) code

A $[[n, K]]$ codeword stabilized code [51] is defined by a stabilizer group \mathcal{S} and a set of n -qubit Pauli-strings, $\mathcal{W} = \{w_k\}_{k=1}^K$, called the word operators. The first word operator w_1 is always chosen to be the identity operator. The code is then spanned by the basis vectors of the form

$$|\psi_{w_k}\rangle = w_k |\psi_s\rangle, \quad (5)$$

where $|\psi_s\rangle$ is the corresponding stabilizer state.

If the stabilizers of the code are in the standard form $X_v Z_{\{n\}}$, then one can transform the word operators to the standard form, strings of Z s. Additionally, any single qubit error acting on the codewords $\{|\psi_{w_k}\rangle\}$ is equivalent to another (possibly multi-qubit) error consisting only of Z s. Since all errors become Z s, one can treat this as a classical error model and find the set of errors that can be detected by the CWS code (see Theorem 3 of Ref. [51]).

The CWS code is a $[[n, k = \log_2 K]]$ stabilizer code (see Theorem 5 of Ref. [51]) if the word operators \mathcal{W} form an abelian group. It should be noted that in general the word operators do not form a group.

III. METHOD AND RESULTS

In this section, we present the details of the classical algorithm to find the best classical state to approximate ground states and present results from different numerical simulations.

A. Stabilizer Configuration Interaction

Inspired by the full configuration interaction (FCI) method, we propose a method to generate stabilizer approximations of ground states by a linear superposition of configurations (excitations). We now describe the describe the method in detail.

1. Reference state

The starting point of our method is choosing a reference state, from which subsequent excitations can be generated. The Hartree-Fock (HF) state (Sec. II A) is chosen as the reference state in our method. It is the best product state approximation to the ground state of the system, as it captures the essential mean-field characteristics of the electronic structure. The HF state, being a stabilizer state, allows us to generate and manage excitations systematically.

2. Excitations

Next, we introduce different excitations in the reference state to create a state that capture the effects of electron correlation (similar to FCI wavefunction (II A)) and improve the stabilizer approximation. We generate these excitations carefully to preserve the stabilizer nature of the resulting state while also maintaining the symmetry of the physical system.

We select a set of operators $\{E_1, E_2, E_3, \dots\}$ to include excitations in the reference state iteratively, as:

$$|\psi_{i+1}\rangle = \frac{(\mathcal{I} + (-1)^l E_{i+1}) |\psi_i\rangle}{\sqrt{2}}, \quad (6)$$

where $l \in \{0, 1\}$ and $|\psi_0\rangle = |\text{HF}\rangle$. The final state $|\psi_n\rangle$ generated by a set of operators $\{E_1, E_2, \dots, E_n\}$ is a stabilizer state with the same symmetry as the reference state if the following conditions are satisfied:

1. Any operator, E_i , acts on equal number of occupied and unoccupied orbitals and excites particles to the same spin orbitals and is of the form $X_{\{o\}}X_{\{u\}}$, where $\{o\}$ and $\{u\}$ represent the set of occupied and unoccupied spin orbitals, respectively.
2. The number of independent single excitation generators $\{X_{o_1}X_{u_1}, \dots, X_{o_m}X_{u_m}\}$ is less than or equal to the number of particles, i.e., $m \leq n_e$, where o_i and u_i are orbitals with the same spin symmetry. Further, any two independent single excitation generators $X_{o_i}X_{u_i}$ and $X_{o_j}X_{u_j}$ are fully disjoint, i.e., $X_{o_i}X_{u_i} \cap X_{o_j}X_{u_j} = \emptyset$.

One can check that if the above conditions are met, that $\langle \psi_{i-1} | E | \psi_{i-1} \rangle = 0$, thus the new state $|\psi_{i+1}\rangle$ (Eq. 6) is a stabilizer state (see Sec. II B). So, if we select the reference state to be a stabilizer state, the final state will also be a stabilizer state.

It should be noted that using such a set of operators one can generate a maximum of 2^{n_o} excitations, which is much lower than the total number of excitations, $2^{n_o+n_u}$, as $n_u \gg n_o$ in many practically relevant cases.

The procedure to generate a set of valid excitation generators is summarized below. First, we construct two matrices corresponding to the two spin excitation generators (alpha and beta), each of size $n_o/2 \times n_u/2$, where n_o and n_u are the number of occupied and virtual (unoccupied) orbitals, respectively. Every element of the matrix holds the corresponding orbital indices, (o_i, u_j) , such that the action of the operator $X_{o_i}X_{u_j}$ on the reference state generates the corresponding single excitation.

We then sample n_o elements $\{(o_{i_1}, u_{j_1}), (o_{i_2}, u_{j_2}), \dots, (o_{i_{n_o}}, u_{j_{n_o}})\}$ from the two matrices, such that no two entries belong to the same row or column. A set of excitation generators is constructed using the single excitation generators $X_{o_i}X_{u_j}$ corresponding to each of the

sampled elements (o_i, u_j) . The number of different excitation generators in the set can vary from 1 to n_o .

3. Algorithm

Given a molecular Hamiltonian, $H = \sum h_i P_i$, and the corresponding Hartree-Fock state $|\psi_0\rangle$. We now describe the procedure for finding stabilizer approximations to ground states of the molecule:

1. Generate all valid sets of excitation generators by following the procedure mentioned above.
2. For every set $\{E_1, E_2, E_3, \dots\}$ generate stabilizer states iteratively using the Hartree-Fock state as the reference state, following the Eq. 6.
3. Calculate the ground state energy corresponding to the molecular Hamiltonian and output the state, $|\psi_n\rangle$, that has the lowest energy.

The above algorithm looks at all the stabilizer states with real amplitudes and only outputs the state with the lowest energy. While energy is the primary metric considered here, one can choose other metrics (similarity, overlap, etc.) and find the best stabilizer state that satisfies the chosen criterion.

B. Adaptive stabilizer CI

The number of valid excitation generator sets grows combinatorially with both the number of occupied orbitals, n_o , and number of unoccupied orbitals, n_u . This growth is manageable for smaller molecules but can become computationally challenging as the system size increases. Taking inspiration from adaptive methods, such as the ones proposed in Refs. [28–31], we propose a method that adaptively includes excitations of higher order and overcomes the scaling problem.

The modified algorithm is described in detail below.

1. Construct a set of all valid double excitation generators of the form X_oX_u , where (o, u) is a pair of orbitals with the same spin, with one being occupied and the other unoccupied.
2. Generate all the stabilizer state of the form:

$$|\psi_{i+1}\rangle = \frac{(\mathcal{I} + (-1)^l X_oX_u) |\psi_i\rangle}{\sqrt{2}}, \quad (7)$$

and $|\psi'_{i+1}\rangle = X_oX_u |\psi_i\rangle$, where $l \in \{0, 1\}$.

3. Select the state(s) $|\psi_{i+1}\rangle$ with the lowest energy and remove the orbitals $\{o, u\}$ involved in the excitation included in $|\psi_{i+1}\rangle$ from consideration in the next steps.

4. Repeat steps 1-3, until all particles have been considered for an excitation.

The above procedure scales as $\mathcal{O}(n^3)$, where $n = n_o + n_u$ is the total number of qubits and allows for investigating larger systems.

C. State preparation circuits

In this section, we present the steps to construct the stabilizer states discussed in the previous sections. It should be noted that there exists a Clifford circuit, \mathcal{C} , such that any stabilizer state $|\psi_s\rangle$ can be constructed by the action of \mathcal{C} on $|0\rangle^{\otimes n}$, i.e., $|\psi_s\rangle = \mathcal{C}|0\rangle^{\otimes n}$. However, this circuit can be quite complex, so we propose an alternative construction based on the Hadamard test protocol [58], that uses additional ancilla qubits and measurement to prepare the desired state.

Given a n -qubit stabilizer state $|\psi_s\rangle = (\mathcal{I} + (-1)^l E)|\psi'_s\rangle/\sqrt{2}$, where E is a Pauli-string of only X s and ψ'_s is another n -qubit stabilizer state, we now construct an unitary, U , on $n + 1$ -qubit, such that $U|\psi'_s\rangle = |\psi_s\rangle$. If the excitation generator E is of the form $X_{k_1}X_{k_2}\dots$, the unitary, U , is:

$$U = H(a) \left(\prod_{k_1, k_2, \dots} \text{CNOT}(a, k_i) \right) H(a), \quad (8)$$

where $H(a)$ is the Hadamard gate acting on the ancilla qubit- a and $\text{CNOT}(a, k_i)$ is the Controlled-NOT gate with a being the control qubit and k_i being the target qubit. A schematic depiction of U is shown in Fig. 1. It can be seen that $U(|0\rangle \otimes |\psi'_s\rangle) = 1/\sqrt{2}\{|0\rangle \otimes [(\mathcal{I} + E)|\psi'_s\rangle/\sqrt{2}] + |1\rangle \otimes [(\mathcal{I} - E)|\psi'_s\rangle/\sqrt{2}]\}$, which upon measuring the ancilla qubit results in the state, $|\psi\rangle = |l\rangle \otimes |\psi_s\rangle = |l\rangle \otimes (\mathcal{I} + (-1)^l E)|\psi'_s\rangle/\sqrt{2}$, where l is the measurement outcome of the ancilla qubit.

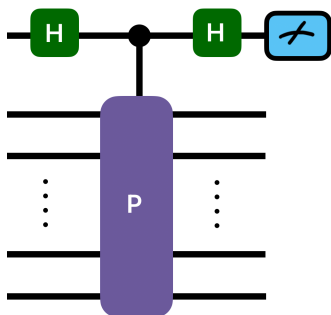


Figure 1. An illustration of the circuit that can be used to prepare a stabilizer state. The purple box labeled “P” represents a multi-qubit Pauli gate and the green boxes labeled “H” represent the Hadamard gate.

We note that using unitaries of the form in Eq. 8 one can generate any stabilizer state of the form in Eq. 6 or Eq. 7.

D. Generalized stabilizer states

We can further modify the best stabilizer states ($1/\sqrt{2}(\mathcal{I} + (-1)^l E)|\psi'_s\rangle$) by allowing for arbitrary amplitudes when forming the superposition as follows:

$$|\psi_s\rangle = (x\mathcal{I} + y(-1)^l E)|\psi'_s\rangle, \quad (9)$$

where x and y are real amplitudes and $x^2 + y^2 = 1$. We do this by adding an extra gate, a single qubit rotation gate around the Y-axis, $R_y(\theta)$ (depicted by the orange box in Fig. 2) on the ancilla qubit. The parameter, θ , can be optimized to minimize the energy corresponding to the state.

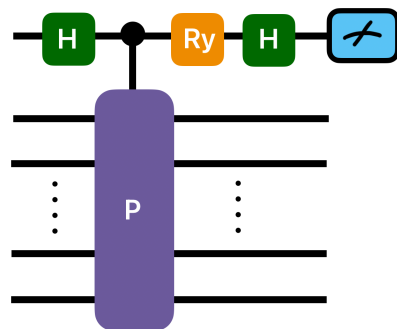


Figure 2. An illustration of the circuit that can be used to prepare a generalized stabilizer state. The purple box labeled “P” represents a multi-qubit Pauli gate, the green boxes labeled “H” represent the Hadamard gate and the orange box labeled “Ry” represents a Ry gate (rotation around the Y-axis).

We use full stabilizer CI algorithm (Sec. III A) for finding the stabilizer approximation to the ground state of these molecules. We also find the generalized stabilizer states corresponding to the best stabilizer states by following the procedure in Sec. III D. The results from the different numerical experiments are presented in Fig. 3 and Fig. 4.

E. Results

In this section, we present the result from various numerical simulations carried to find stabilizer approximation for different molecules. We use the python packages *tequila* [59], *stim* [60] and *cirq* [61] to perform the various calculations.

First we use the stabilizer CI (Sec. III A) method for small molecules, followed by the adaptive stabilizer method (Sec. III B) for larger molecules and report the results next. All energy values are in Hartree (Ha) units and all bond length values are in Angstrom (Å) units, unless specified otherwise.

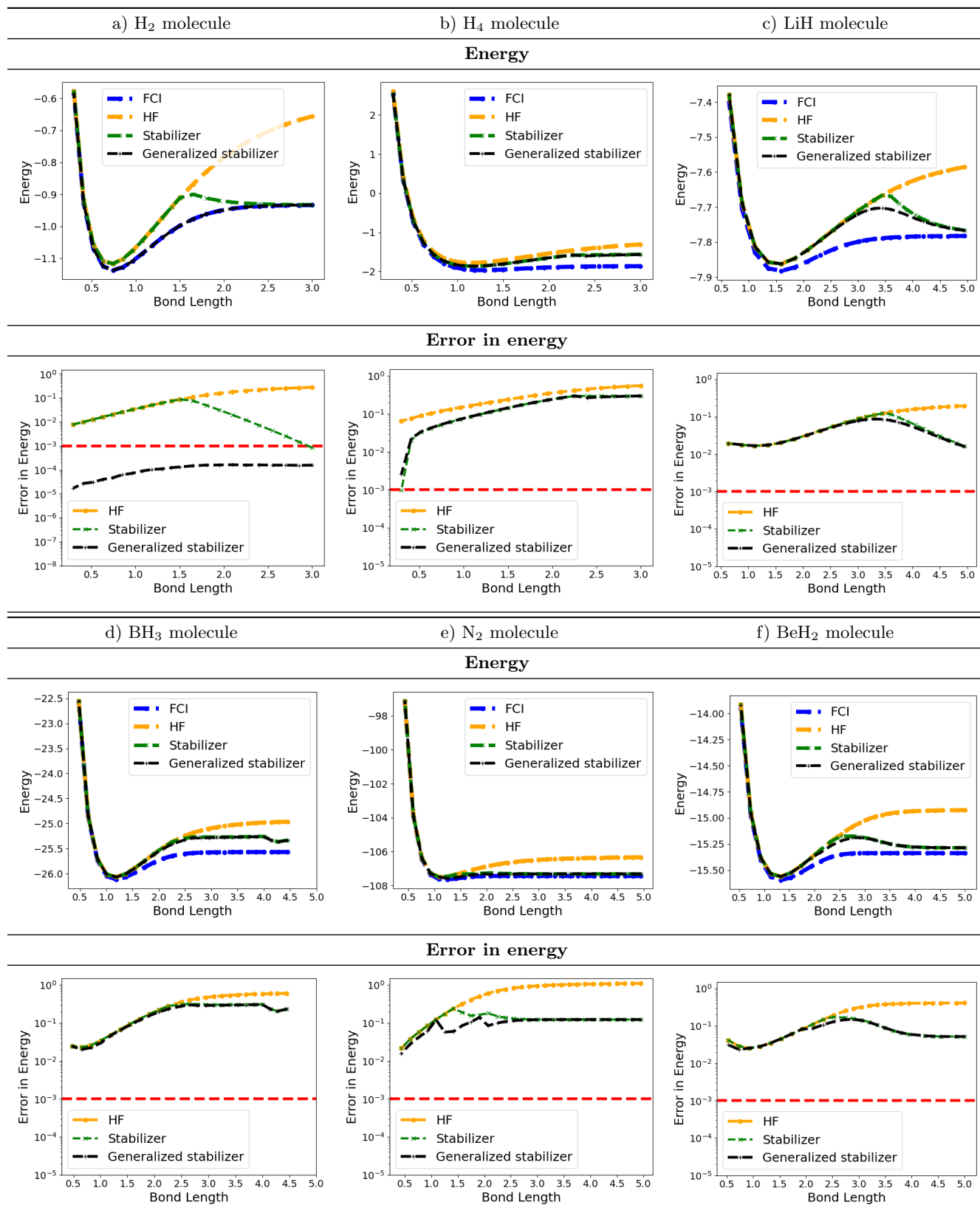


Figure 3. A plot showing the potential energy surface (top) and error when compared to the FCI energy (bottom) for different molecules considered in this study. The red line denotes an error value of $1mHa$.

1. Small molecules

We consider different commonly studied small molecules in the minimal basis (STO-3G), such as H_2 , LiH , H_4 , BH_3 , BeH_2 and N_2 . The details of the different molecules are summarized in Table I.

Molecule	Number of Electrons	Number of Qubits
H_2	2(2)	4(4)
LiH	4(4)	12(12)
H_4	4(4)	8(8)
N_2	6(14)	12(20)
BeH_2	6(6)	14(14)
BH_3	6(8)	12(16)

Table I. A table containing the details of the different molecules considered here. The numbers correspond to the used (total) number of electrons/qubits, respectively.

It can be seen from Fig. 3, that the HF state is a pretty good approximation to the actual ground state in configurations close to the equilibrium geometry of the molecules. However, they tend to perform worse for stretched configurations far from equilibrium, which is the expected, because of the lack of electronic correlations in these states.

The stabilizer state with the lowest energy in configurations close to the equilibrium geometry of the molecules is the HF state [25, 26] and the proposed stabilizer CI method also identifies this state as the optimal stabilizer approximation. However, for the case of the Hydrogen ring (H_4 molecule - Fig. 3 b), we observe that the stabilizer state with the lowest energy is not the HF state, but an entangled state.

In stretched configurations far from equilibrium, the proposed method finds entangled stabilizer states as the best stabilizer approximation. These states capture some of the electronic correlations and thus have energies closer to the true ground state. We see close to an order magnitude reduction in error when compared to the HF state, for all molecules in highly stretched configurations. In certain cases (H_4 and H_2 molecule), the energy corresponding to these states are well within the chemical accuracy (error < 1 mHa).

Finally, it should be noted that the generalized stabilizer state is better approximation to the ground state than the stabilizer state, as it allows for a biased superposition of some excitations. In case of H_2 molecule, (Fig. 3 a) the generalized stabilizer state is a very good approximation (error < 1 mHa) to the true ground state for all configurations. This high accuracy is due to the fact that both the true ground state and the optimal stabilizer state share the same configuration. By removing the unbiased restriction inherent in stabilizer states, we can optimize the amplitudes, thereby bringing the approximation closer to the true ground state.

This is not the case for all other molecules and the generalized stabilizer state only leads to small improvements in energy. Nonetheless, this provides evidence that stabilizer states with similar configuration to the ground state can be a good starting point for finding ground states.

2. Larger molecules

We now report the result for two slightly larger molecules C_2H_6 and Cr_2 in the minimal (STO-3G) basis. We consider an active space of 28 qubits (14 occupied (electrons) and 14 unoccupied spin orbitals) for the C_2H_6 and 36 qubits (12 occupied (electrons) and 24 unoccupied spin orbitals) for the Cr_2 molecule. These molecules are significantly larger than the ones considered in Sec. III E 1, thus we do not use the full stabilizer CI algorithm (Sec. III A) but the adaptive stabilizer CI algorithm (Sec. III B) for finding the stabilizer approximation to the ground state of these molecules. We plot the result from the numerical experiments in Fig. 4.

We plot the results for molecular geometries where the bond length exceeds twice the equilibrium geometry, as it is well-known that the Hartree-Fock (HF) state performs poorly in these regions. As shown in Fig 4, the best stabilizer states (see the Appendix V C for some examples) consistently achieve lower energies compared to the HF state. This behavior is similar to our observations for smaller molecules, where introducing excitations to the HF state improves the approximation as they capture electronic correlations.

These results suggest that stabilizer states can serve as reliable approximations to the true ground states of molecules, providing a better starting point for more complex simulations, such as VQE [20] or QPE [17, 18], in situations where the HF state is not a good approximation.

IV. ERROR DETECTION

In this section, we provide a detailed description of the procedure for constructing the codes and demonstrate their error-detection capabilities.

We first note that any state $|\psi\rangle$ that we construct as an approximation of the ground state in this study (using Eq. 6 or Eq. 7) is a stabilizer state. Thus, there exist a set of operators \mathcal{S} , such that $s_i |\psi\rangle = |\psi\rangle \forall s_i \in \mathcal{S}$. The exact procedure to construct the stabilizers is presented in detail in the Appendix (V A).

Next, we outline the procedure of constructing a error detection code which can be used to prepare the state $|\psi\rangle$.

1. Given the stabilizers \mathcal{S} of the state $|\psi\rangle$, find the local Clifford unitary, \mathcal{C} , that converts it to the

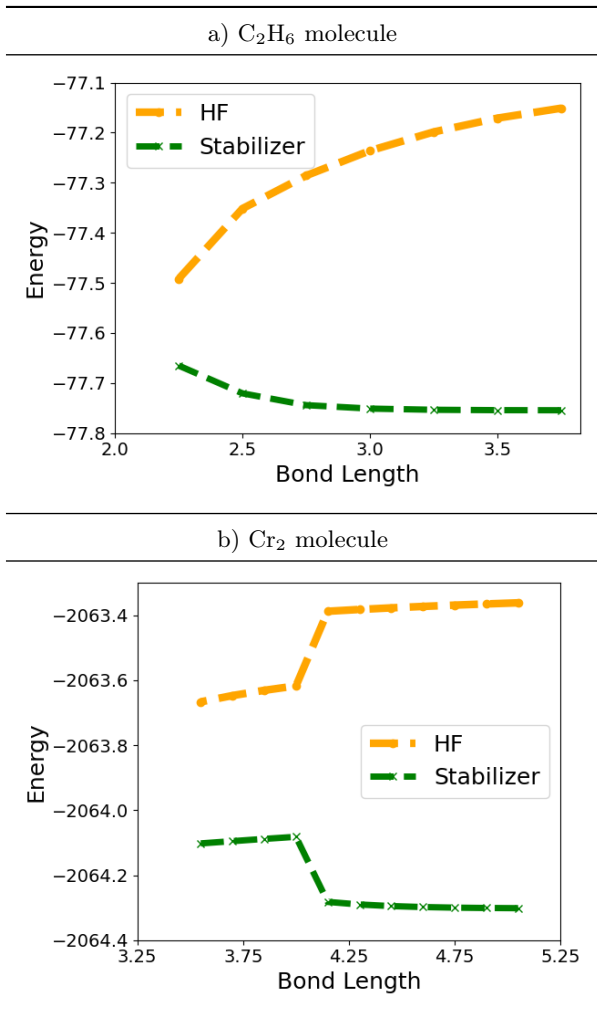


Figure 4. A plot showing the energy values of the Hartree-Fock state and best stabilizer state for different bond length of the C_2H_6 and Cr_2 molecule.

standard form, \mathcal{S}' . [25, 55, 56]

2. Construct the error characterization table for this stabilizer group and find the operators (abelian) that can be used as word operators, \mathcal{W} . (see Appendix VB for details)
3. Define a Codeword stabilized (CWS) code using the word operators, \mathcal{W} , and the stabilizers, \mathcal{S}' .
4. Find the equivalent stabilizer code as follows:
 - (a) Fix one of the non-trivial word operator, w_i , to be the logical- X operator.
 - (b) Find a stabilizer $s_i \in \mathcal{S}'$ that anti-commutes with, w_i , and fix it to be the logical- Z operator.
 - (c) Remove s_i from \mathcal{S}' and modify the remaining stabilizers to get a set of stabilizers \mathcal{S}'' ,

so that every remaining stabilizer commutes with w_i and s_i .

- (d) The stabilizers \mathcal{S}'' , logical- $X = w_i$ and logical- $Z = s_i$ operators, define the equivalent stabilizer code.

We use the above procedure to construct some error detection codes for different molecules studied in paper and present them in the Appendix (VC). The resulting code can be used to prepare the best stabilizer state $|\psi\rangle$ of the form in Eq. 6 or Eq. 7 with error detection on a physical device and post-selection, as the state $|\psi\rangle$ is a logical basis state of the code.

In certain cases (usually states with more than 2 excitations), we observe that some generalized stabilizer state (of the form in Eq. 9) can also be prepared while detecting errors and using post-selection. This is possible because in these cases, the generalized state are the arbitrary superposition of the logical states, ($|\bar{0}\rangle$ and $|\bar{1}\rangle$) or ($|\bar{+}\rangle$ and $|\bar{-}\rangle$). Thus, using protocols that allow for universal quantum computations, such as magic state distillation [62], we can also prepare these states with the codes. Some examples of such states are presented in the Appendix (VD).

This suggests that if the code we construct can have more logical states with the same symmetry as that of the molecule, we can prepare more generalized stabilizer states.

Next, we carry out numerical simulations with noise to demonstrate the preparation of a (generalized) stabilizer state for the case of H_4 molecule using the codes we construct, which are listed in the Appendix VC. We prepare a stabilizer state, $|\psi_s\rangle$,

$$|\psi_s\rangle = \frac{1}{2}(|11110000\rangle - |11000011\rangle - |00111100\rangle + |00001111\rangle),$$

and an arbitrary generalized stabilizer state, $|\psi'_s\rangle$,

$$|\psi'_s\rangle = 0.3928|11110000\rangle - 0.5879|11000011\rangle - 0.5879|00111100\rangle + 0.3928|00001111\rangle.$$

To perform noisy simulation, we use a simple noise model, where we add a depolarizing channel after state preparation circuit and bit-flip channel before stabilizer measurement. An illustration of the circuits used in these simulation is shown in Fig. 5. The gates marked in red color represent the depolarizing channel on the data qubits and bit-flip channel on the ancilla qubits. In all the simulations, we fixed bit-flip probability to be half the depolarizing probability. All other operations in these circuits are ideal. The actual circuit is shown in the Appendix VE.

Using the circuits in Fig. 5, we prepare noisy states and calculate the overlap with the ideal states for different error probabilities. In the noisy simulations, with

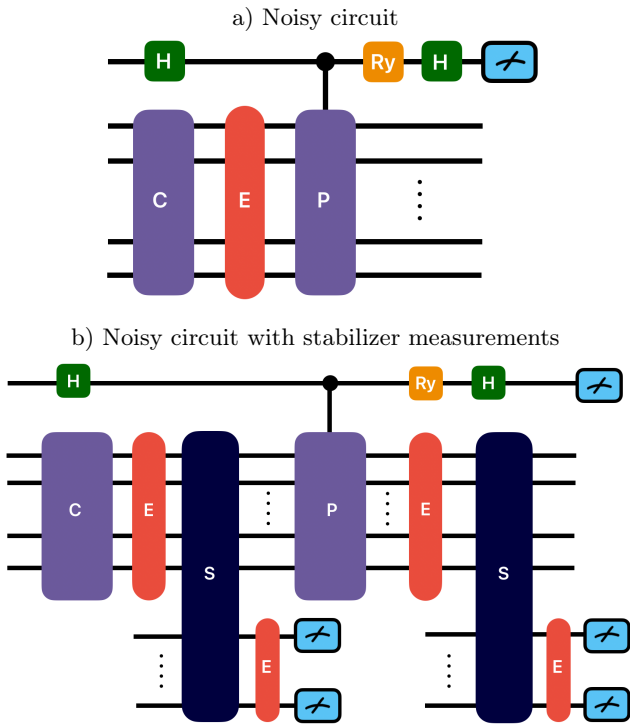


Figure 5. Illustration of circuits used for noisy preparation of a (generalized) stabilizer state in the case of the H_4 molecule. The purple boxes labeled “C” and “P” represent a Clifford circuit and multi-qubit Pauli gate, respectively. The green boxes labeled “H” represent the Hadamard gate, the orange box labeled “Ry” represents a Ry gate (rotation around the Y-axis), the dark blue boxes labeled “S” represent the stabilizer extraction circuit and the red boxes labeled “E” represent the error (depolarizing or bit-flip) channel.

and without error detection, we use 1000 different repetitions of the circuits to calculate the average overlap. In the noisy simulations with stabilizer measurements, we discard any state if we detect any error. The results from these simulations are plotted in Fig. 6.

In simulations without error detection, we observe that the overlap decreases exponentially as a function of the error probability. Using error detection, we achieve a higher overlap compared to unprotected noisy operations, albeit at the cost of an increasing discard rate as the error probability rises. However, it should be noted that for error probabilities below 0.01, the overlap remains close to 1, with a discard rate of less than 20%. Therefore, our proposal can be particularly useful in these regimes.

V. CONCLUSION

We have proposed a novel framework for finding molecular subspaces with error detection properties by integrating the design of algorithms and error detection

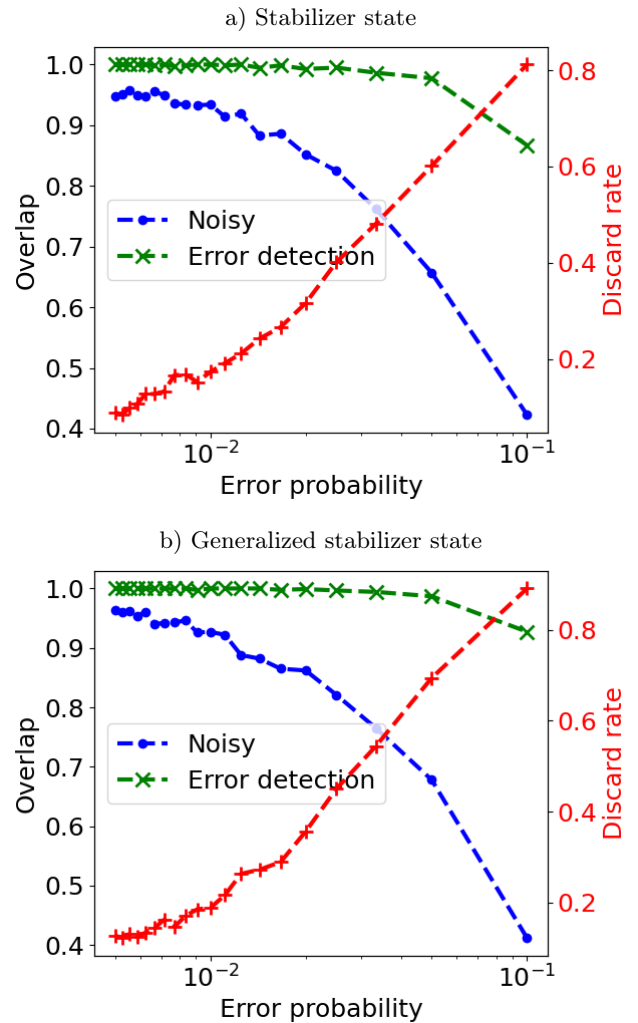


Figure 6. A plot comparing the overlap of noisy states with the ideal state from simulations with and without and error detection as a function of the depolarizing error probability. The red line represents the discard rate for the simulations with error detection.

codes. By focusing on ground state approximation, we developed efficient classical algorithms for constructing stabilizer approximations to the ground states of various molecules. Additionally, we introduced circuit constructions for preparing generalized stabilizer states.

We then use the stabilizer approximations to construct quantum error detection codes using codeword stabilized codes. These codes require minimal resources and facilitate state preparation with error detection for both stabilizer and some generalized stabilizer states.

We also conduct various numerical experiments to verify the proposed method by investigating molecules up to 36 qubits. We observe that the stabilizer states outperform the Hartree-Fock state in every case. However, while they do not yet achieve the desired accuracy for most molecules studied, we find that these stabilizer

states can serve as a promising starting point for further complex calculations.

Using noisy numerical simulations, we verify the error detection properties of the codes we construct for preparing both a stabilizer and a generalized stabilizer state. These simulations suggest that our method can be useful in preparing approximate eigenstates for different molecular systems, albeit with a measurement overhead due to increasing discard rates.

This work represents an initial step toward algorithms suitable for implementation on early fault-tolerant quantum devices, with a focus on single stabilizer states. We anticipate that employing linear combinations [63] of different stabilizer states could yield better ground state approximations, similar to studies using superposition

of spin-coupled states [64] for accurate ground state energies. Further research is needed to explore this approach and develop fault-tolerant protocols for preparing these states. Future work will also examine the error-correction properties of different physical Hamiltonians.

ACKNOWLEDGEMENTS

The authors thank Andrew Nemeč and Bálint Pató for helpful discussions. This work was supported by the National Science Foundation (NSF) Quantum Leap Challenge Institute of Robust Quantum Simulation (QLCI grant OMA-2120757).

-
- [1] G. Q. AI., *Nature* **614**, 676 (2023).
- [2] S. Krinner, N. Lacroix, A. Remm, A. Di Paolo, E. Genois, C. Leroux, C. Hellings, S. Lazar, F. Swiadek, J. Herrmann, *et al.*, *Nature* **605**, 669 (2022).
- [3] C. K. Andersen, A. Remm, S. Lazar, S. Krinner, N. Lacroix, G. J. Norris, M. Gabureac, C. Eichler, and A. Wallraff, *Nature Physics* **16**, 875 (2020).
- [4] D. Bluvstein, S. J. Evered, A. A. Geim, S. H. Li, H. Zhou, T. Manovitz, S. Ebadi, M. Cain, M. Kalinowski, D. Hangleiter, *et al.*, *Nature* **626**, 58 (2024).
- [5] C. Ryan-Anderson, J. G. Bohnet, K. Lee, D. Gresh, A. Hankin, J. Gaebler, D. Francois, A. Chernoguzov, D. Lucchetti, N. C. Brown, *et al.*, *Physical Review X* **11**, 041058 (2021).
- [6] L. Egan, D. M. Debroy, C. Noel, A. Risinger, D. Zhu, D. Biswas, M. Newman, M. Li, K. R. Brown, M. Cetina, *et al.*, *Nature* **598**, 281 (2021).
- [7] L. Postler, S. Heuβen, I. Pogorelov, M. Rispler, T. Feldker, M. Meth, C. D. Marciniak, R. Stricker, M. Ringbauer, R. Blatt, *et al.*, *Nature* **605**, 675 (2022).
- [8] A. Katabarwa, K. Gratsea, A. Caesura, and P. D. Johnson, *PRX Quantum* **5**, 020101 (2024).
- [9] E. T. Campbell, *Quantum Science and Technology* **7**, 015007 (2021).
- [10] L. Lin and Y. Tong, *PRX Quantum* **3**, 010318 (2022).
- [11] Z. Ding and L. Lin, *PRX Quantum* **4**, 020331 (2023).
- [12] R. Zhang, G. Wang, and P. Johnson, *Quantum* **6**, 761 (2022).
- [13] V. Kliuchnikov, K. Lauter, R. Minko, A. Paetznic, and C. Petit, *Quantum* **7**, 1208 (2023).
- [14] V. Vandaale, arXiv preprint arXiv:2407.08695 (2024).
- [15] A. Kissinger and J. van de Wetering, arXiv preprint arXiv:1903.10477 (2019).
- [16] J. S. Nelson and A. D. Baczewski, arXiv preprint arXiv:2403.00077 (2024).
- [17] A. Aspuru-Guzik, A. D. Dutoi, P. J. Love, and M. Head-Gordon, *Science* **309**, 1704 (2005).
- [18] D. S. Abrams and S. Lloyd, *Physical Review Letters* **79**, 2586 (1997).
- [19] A. Anand, P. Schleich, S. Alperin-Lea, P. W. Jensen, S. Sim, M. Diaz-Tinoco, J. S. Kottmann, M. Degroote, A. F. Izmaylov, and A. Aspuru-Guzik, *Chemical Society Reviews* **51**, 1659 (2022).
- [20] A. Peruzzo, J. McClean, P. Shadbolt, M.-H. Yung, X.-Q. Zhou, P. J. Love, A. Aspuru-Guzik, and J. L. O’Brien, *Nature communications* **5**, 4213 (2014).
- [21] M. Motta, C. Sun, A. T. Tan, M. J. O’Rourke, E. Ye, A. J. Minnich, F. G. Brandao, and G. K.-L. Chan, *Nature Physics* **16**, 205 (2020).
- [22] S. McArdle, T. Jones, S. Endo, Y. Li, S. C. Benjamin, and X. Yuan, *npj Quantum Information* **5**, 75 (2019).
- [23] M. Cerezo, A. Arrasmith, R. Babbush, S. C. Benjamin, S. Endo, K. Fujii, J. R. McClean, K. Mitarai, X. Yuan, L. Cincio, *et al.*, *Nature Reviews Physics* , 1 (2021).
- [24] K. Bharti, A. Cervera-Lierta, T. H. Kyaw, T. Haug, S. Alperin-Lea, A. Anand, M. Degroote, H. Heimonen, J. S. Kottmann, T. Menke, *et al.*, *Reviews of Modern Physics* **94**, 015004 (2022).
- [25] A. Anand and K. R. Brown, arXiv preprint arXiv:2312.17146 (2023).
- [26] A. Anand and K. R. Brown, arXiv preprint arXiv:2312.08502 (2023).
- [27] D. Wecker, M. B. Hastings, and M. Troyer, *Physical Review A* **92**, 042303 (2015).
- [28] H. R. Grimsley, S. E. Economou, E. Barnes, and N. J. Mayhall, *Nature communications* **10**, 3007 (2019).
- [29] I. G. Ryabinkin, T.-C. Yen, S. N. Genin, and A. F. Izmaylov, *Journal of chemical theory and computation* **14**, 6317 (2018).
- [30] I. G. Ryabinkin, R. A. Lang, S. N. Genin, and A. F. Izmaylov, *Journal of chemical theory and computation* **16**, 1055 (2020).
- [31] H. L. Tang, V. Shkolnikov, G. S. Barron, H. R. Grimsley, N. J. Mayhall, E. Barnes, and S. E. Economou, *PRX Quantum* **2**, 020310 (2021).
- [32] J. R. McClean, J. Romero, R. Babbush, and A. Aspuru-Guzik, *New Journal of Physics* **18**, 023023 (2016).
- [33] J. S. Kottmann and A. Aspuru-Guzik, *Physical Review A* **105**, 032449 (2022).
- [34] P. Schleich, J. Boen, L. Cincio, A. Anand, J. S. Kottmann, S. Tretiak, P. A. Dub, and A. Aspuru-Guzik, *Journal of Chemical Theory and Computation* **19**, 4952 (2023).

- [35] A. Anand, J. S. Kottmann, and A. Aspuru-Guzik, arXiv preprint arXiv:2207.02961 (2022).
- [36] G. S. Ravi, P. Gokhale, Y. Ding, W. Kirby, K. Smith, J. M. Baker, P. J. Love, H. Hoffmann, K. R. Brown, and F. T. Chong, in *Proceedings of the 28th ACM International Conference on Architectural Support for Programming Languages and Operating Systems, Volume 1* (2022) pp. 15–29.
- [37] Q. Wang, L. Zhukas, Q. Miao, A. S. Dalvi, P. J. Love, C. Monroe, F. T. Chong, and G. S. Ravi, arXiv preprint arXiv:2408.06482 (2024).
- [38] M. Schuld, V. Bergholm, C. Gogolin, J. Izaac, and N. Killoran, *Physical Review A* **99**, 032331 (2019).
- [39] K. Mitarai, M. Negoro, M. Kitagawa, and K. Fujii, *Physical Review A* **98**, 032309 (2018).
- [40] J. S. Kottmann, A. Anand, and A. Aspuru-Guzik, *Chemical science* **12**, 3497 (2021).
- [41] D. Wierichs, J. Izaac, C. Wang, and C. Y.-Y. Lin, *Quantum* **6**, 677 (2022).
- [42] J. Gacon, C. Zoufal, G. Carleo, and S. Woerner, *Quantum* **5**, 567 (2021).
- [43] A. Anand, M. Degroote, and A. Aspuru-Guzik, *Machine Learning: Science and Technology* **2**, 045012 (2021).
- [44] X. Bonnet-Monroig, H. Wang, D. Vermetten, B. Senjean, C. Moussa, T. Bäck, V. Dunjko, and T. E. O’Brien, *Physical Review A* **107**, 032407 (2023).
- [45] R. Sweke, F. Wilde, J. Meyer, M. Schuld, P. K. Fährmann, B. Meynard-Piganeau, and J. Eisert, *Quantum* **4**, 314 (2020).
- [46] J. R. McClean, S. Boixo, V. N. Smelyanskiy, R. Babbush, and H. Neven, *Nature communications* **9**, 1 (2018).
- [47] M. Cerezo, A. Sone, T. Volkoff, L. Cincio, and P. J. Coles, *Nature communications* **12**, 1 (2021).
- [48] S. Wang, E. Fontana, M. Cerezo, K. Sharma, A. Sone, L. Cincio, and P. J. Coles, *Nature communications* **12**, 1 (2021).
- [49] C. O. Marrero, M. Kieferová, and N. Wiebe, *PRX Quantum* **2**, 040316 (2021).
- [50] J. Sun, L. Cheng, and S.-X. Zhang, arXiv preprint arXiv:2403.08441 (2024).
- [51] A. Cross, G. Smith, J. A. Smolin, and B. Zeng, in *2008 IEEE International Symposium on Information Theory (IEEE, 2008)* pp. 364–368.
- [52] A. Szabo and N. S. Ostlund, *Modern quantum chemistry: introduction to advanced electronic structure theory* (Courier Corporation, 2012).
- [53] T. Helgaker, P. Jorgensen, and J. Olsen, *Molecular electronic-structure theory* (John Wiley & Sons, 2013).
- [54] D. Gottesman, *Stabilizer codes and quantum error correction* (California Institute of Technology, 1997).
- [55] M. Van den Nest, J. Dehaene, and B. De Moor, *Physical Review A* **69** (2004).
- [56] B. Zeng, H. Chung, A. W. Cross, and I. L. Chuang, *Physical Review A* **75**, 032325 (2007).
- [57] H. J. García, I. L. Markov, and A. W. Cross, arXiv preprint arXiv:1711.07848 (2017).
- [58] R. Cleve, A. Ekert, C. Macchiavello, and M. Mosca, *Proceedings of the Royal Society of London. Series A: Mathematical, Physical and Engineering Sciences* **454**, 339 (1998).
- [59] J. S. Kottmann, S. Alperin-Lea, T. Tamayo-Mendoza, A. Cervera-Lierta, C. Lavigne, T.-C. Yen, V. Verteletskyi, P. Schleich, A. Anand, M. Degroote, *et al.*, *Quantum Science and Technology* **6**, 024009 (2021).
- [60] C. Gidney, *Quantum* **5**, 497 (2021).
- [61] C. Developers, *Cirq* (2024).
- [62] S. Bravyi and A. Kitaev, *Physical Review A—Atomic, Molecular, and Optical Physics* **71**, 022316 (2005).
- [63] A. M. Childs and N. Wiebe, arXiv preprint arXiv:1202.5822 (2012).
- [64] D. Marti-Dafcik, N. Lee, H. G. Burton, and D. P. Tew, arXiv preprint arXiv:2402.08858 (2024).

APPENDIX

A. Stabilizers of unbiased sum of stabilizer states

The procedure outlined in this section closely follows Ref. [57].

Given any stabilizer state, $|\psi_i\rangle$, (reference state in Eq. 6 or Eq. 7), there exist a Clifford unitary, \mathcal{C}_i , which maps the state, $|\psi_i\rangle$, to basis from, i.e., $\mathcal{C}_i |\psi_i\rangle = |0\rangle^{\otimes n}$.

It can also be verified that the action of \mathcal{C}_i on $E_{i+1} |\psi_i\rangle$ also produces a basis state, $\mathcal{C}_i E_{i+1} |\psi_i\rangle = \mathcal{C}_i E_{i+1} \mathcal{C}_i^\dagger \mathcal{C}_i |\psi_i\rangle = \mathcal{C}_i E_{i+1} \mathcal{C}_i^\dagger |0\rangle^{\otimes n} = E'_{i+1} |0\rangle^{\otimes n} = i^m |b_1 b_2 \dots b_n\rangle$, where $m \in \{0, 1, 2, 3\}$, $b_i \in \{0, 1\}$ and $E_i, E'_{i+1} \in \mathcal{G}_n$. Thus, the state $|\psi_{i+1}\rangle$ in Eq. 6 or Eq. 7 can be written as:

$$\begin{aligned} |\psi_{i+1}\rangle &= \mathcal{C}_i^\dagger \left(\frac{|0\rangle^{\otimes n} + i^{(2l+m) \bmod 4} |b_1 b_2 \dots b_n\rangle}{\sqrt{2}} \right) \\ &= \mathcal{C}_i^\dagger |\psi_z\rangle |\psi_{\text{GHZ}}\rangle, \end{aligned} \quad (10)$$

where $|\psi_z\rangle$ is an all-zero state supported on qubits, $i \in \{i|b_i = 0\}$ and $|\psi_{\text{GHZ}}\rangle$ is the GHZ state supported on qubits, $i \in \{i|b_i = 1\}$.

The stabilizers of the state $|\psi_{i+1}\rangle$ can then be written as $\mathcal{S} = \mathcal{C}_i^\dagger \langle \mathcal{S}_z, \mathcal{S}_{\text{GHZ}} \rangle \mathcal{C}_i$, where $\mathcal{S}_z = \langle Z_i, i \in \{i|b_i = 0\} \rangle$ and \mathcal{S}_{GHZ} is supported on qubits, $i \in \{i|b_i = 1\}$ and

$$\mathcal{S}_{\text{GHZ}} = \begin{cases} \langle (-1)^{t/2} X X \dots X, \forall i Z_i Z_{i+1} \rangle & \text{if } t = 0 \\ \langle (-1)^{(t-1)/2} Y Y \dots Y, \forall i Z_i Z_{i+1} \rangle & \text{if } t = 1 \end{cases}$$

where $t = ((2l + m) \bmod 4) \bmod 2$.

Also, the Clifford unitary \mathcal{C}_{i+1} that maps $|\psi_{i+1}\rangle$ to basis from, $|0\rangle^{\otimes n}$ can be written as:

$$\mathcal{C}_{i+1} = \mathcal{C}_{\text{GHZ}} \mathcal{C}_i, \quad (11)$$

where \mathcal{C}_{GHZ} is the Clifford unitary that maps the GHZ state $|\psi_{\text{GHZ}}\rangle$ to the state $|0\rangle^{\otimes m}$.

B. Error characterization table and word operators

Given a set of stabilizers, \mathcal{S} , in the standard form, i.e., every element s_i is of the form $X_{u_i} Z_{\{v_i\}}$, where, u_i is an integer and $\{v_i\}$ is a set of integers. It can be noted that any single qubit error is equivalent to an error-string of only Zs. This can be seen by representing them in a tabular form, which we refer to as the error-characterization table (see Table V B).

Error \ Qubit	1	2	...	n
X_i	$Z_{\{v_1\}}$	$Z_{\{v_2\}}$...	$Z_{\{v_n\}}$
Y_i	$Z_1 Z_{\{v_1\}}$	$Z_2 Z_{\{v_2\}}$...	$Z_n Z_{\{v_n\}}$
Z_i	Z_1	Z_2	...	Z_n

Table II. An illustration of the error characterization table.

There are $2^n - 1$ distinct Pauli operators of only Zs and at-most $3n$ different single qubit errors. Thus, for $n > 3$, there exists an operator, w , that is not present in the error characterization table. The set of operators, $\{\mathcal{I}, w\}$, along with the stabilizers, \mathcal{S} , can be used to construct a codeword stabilizer code.

C. Example stabilizer states and corresponding codes

In this section, we present some example quantum error detection codes for preparing stabilizer ground state approximations of different molecules that were considered in this study.

1. H_2 molecule

The stabilizer state, $|\psi_s\rangle$, with the lowest energy at bond length 3.0\AA is,

$$|\psi_s\rangle = \frac{1}{\sqrt{2}}(|1100\rangle - |0011\rangle).$$

The stabilizers for this state are

$$\mathcal{S} = \{-Z_1Z_3, -Z_2Z_4, Z_3Z_4, -X_1X_2X_3X_4\}.$$

Using the operators $\{\mathcal{I}, Z_3Z_4\}$ as word operators, the resulting stabilizer code is a $[[4,1,2]]$ code and has the following logical operators, $\bar{Z} = Z_3Z_4$, $\bar{X} = -X_1X_3$, and the following stabilizers, $\mathcal{S}' = \{-Z_1Z_3, -Z_2Z_4, -X_1X_2X_3X_4\}$. It can be verified that the state, $|\psi_s\rangle$, is in the codespace of the above stabilizer code.

2. H_4 molecule

The stabilizer state, $|\psi_s\rangle$, with the lowest energy at bond length 3.0\AA is,

$$|\psi_s\rangle = \frac{1}{2}(|11110000\rangle - |11000011\rangle - |00111100\rangle + |00001111\rangle).$$

The stabilizer code for the above state is a $[[8, 1, 2]]$ code and has the following logical operators, $\bar{X} = Z_6Z_8$, $\bar{Z} = -X_1X_2X_5X_6$, and the following stabilizers, $\mathcal{S}' = \{-Z_1Z_6, -Z_2Z_6, -Z_3Z_8, -Z_4Z_8, Z_5Z_6, Z_7Z_8, X_1X_2X_3X_4X_5X_6X_7X_8\}$.

3. BH_3 molecule

The stabilizer state, $|\psi_s\rangle$, with the lowest energy at bond length 4.45\AA is,

$$|\psi_s\rangle = \frac{1}{\sqrt{8}}(|111111000000\rangle + |110000111100\rangle + |110100111000\rangle - |111000110100\rangle - |110011001100\rangle - |111100110000\rangle - |110111001000\rangle + |111011000100\rangle).$$

The stabilizer code for the above state is a $[[12, 1, 2]]$ code and has the following logical operators, $\bar{X} = Z_8Z_9$, $\bar{Z} = -X_5X_6X_7X_8$, and the following stabilizers, $\mathcal{S}' = \{-Z_1, -Z_2, -Z_3Z_9, -Z_4Z_{10}, -Z_5Z_8, -Z_6Z_8, Z_7Z_8, X_3X_9, X_4X_{10}, Z_{11}, Z_{12}\}$.

4. BeH_2 molecule

The stabilizer state, $|\psi_s\rangle$, with the lowest energy at bond length 3.0\AA is,

$$|\psi_s\rangle = \frac{1}{\sqrt{2}}(|11111100000000\rangle - |11110011000000\rangle).$$

The stabilizer code for the above state is a $[[14, 1, 2]]$ code and has the following logical operators, $\bar{Z} = Z_7Z_8$, $\bar{X} = -X_5X_7$, and the following stabilizers, $\mathcal{S}' = \{-Z_1, -Z_2, -Z_3, -Z_4, -Z_5Z_7, -Z_6Z_8, -X_5X_6X_7X_8, Z_9, Z_{10}, Z_{11}, Z_{12}, Z_{13}, Z_{14}\}$.

5. C_2H_6 molecule

The stabilizer state, $|\psi_s\rangle$, with the lowest energy at bond length 3.75\AA is,

$$|\psi_s\rangle = \frac{1}{2}(|11111111111111000000000000\rangle - |1111111111110011000000000000\rangle - |111111111110011001100000000000\rangle + |111111111110000111100000000000\rangle).$$

The stabilizer code for the above state is a $[[28, 1, 2]]$ code and has the following logical operators, $\bar{X} = Z_{16}Z_{18}$, $\bar{Z} = -X_{10}X_{11}X_{14}X_{15}$, and the following stabilizers, $\mathcal{S}' = \{-Z_1, -Z_2, -Z_3, -Z_4, -Z_5, -Z_6, -Z_7, -Z_8, -Z_9, -Z_{10}Z_{15}, -Z_{11}Z_{15}, -Z_{12}Z_{17}, -Z_{13}Z_{17}, Z_{14}Z_{15}, Z_{16}Z_{17}, X_{10}X_{11}X_{12}X_{13}X_{14}X_{15}X_{16}X_{17}, Z_{18}, Z_{19}, Z_{20}, Z_{21}, Z_{22}, Z_{23}, Z_{24}, Z_{25}, Z_{26}, Z_{27}, Z_{28}\}$.

6. Cr_2 molecule

The stabilizer state, $|\psi_s\rangle$, with the lowest energy at bond length 5.05Å is,

$$\begin{aligned} |\psi_s\rangle = & \frac{1}{4}(|11111111111100000000000000000000\rangle - |111111111100000000001100000000000000\rangle \\ & - |111111110011000000000011000000000000\rangle + |111111110000000000001111000000000000\rangle \\ & + |11111010111100000000000000000010001\rangle - |111110101100000000001100000000010001\rangle \\ & - |111110100011000000000011000000010001\rangle + |111110100000000000001111000000010001\rangle \\ & + |111101011111000000000000000010001000\rangle - |111101011100000000001100000010001000\rangle \\ & - |111101010011000000000011000010001000\rangle + |111101010000000000001111000010001000\rangle \\ & + |111100001111000000000000000010011001\rangle - |111100001100000000001100000010011001\rangle \\ & - |111100000011000000000011000010011001\rangle + |111100000000000000001111000010011001\rangle) \end{aligned}$$

The stabilizer code for the above state is a $[[36, 1, 2]]$ code and has the following logical operators, $\bar{X} = Z_{22}Z_{24}$, $\bar{Z} = -X_{11}X_{12}X_{21}X_{22}$, and the following stabilizers, $\mathcal{S}' = \{-Z_1, -Z_2, -Z_3, -Z_4, -Z_5Z_{33}, -Z_6Z_{36}, -Z_7Z_{33}, -Z_8Z_{36}, -Z_9Z_{24}, -Z_{10}Z_{24}, -Z_{11}Z_{22}, -Z_{12}Z_{22}, Z_{21}Z_{22}, Z_{23}Z_{24}, Z_{29}Z_{33}, Z_{31}Z_{36}, X_6X_8X_{32}X_{36}, X_5X_7X_{29}X_{33}, X_9X_{10}X_{23}X_{24}, Z_{13}, Z_{14}, Z_{15}, Z_{16}, Z_{17}, Z_{18}, Z_{19}, Z_{20}, Z_{25}, Z_{26}, Z_{27}, Z_{28}, Z_{30}, Z_{31}, Z_{34}, Z_{35}\}$.

D. Example preparation of generalized stabilizer states

In this section we present some examples of generalized stabilizer states for the different molecules considered in this study that can be prepared using the error-detection codes.

1. H_4 molecule

The stabilizer state, $|\psi_s\rangle$, with the lowest energy at bond length 3.0Å is,

$$|\psi_s\rangle = \frac{1}{2}(|11110000\rangle - |11000011\rangle - |00111100\rangle + |00001111\rangle).$$

The logical states, $|\bar{\pm}\rangle$, of the code for this state in Sec. VC-2., are $|\alpha\rangle = 1/\sqrt{2}(|11110000\rangle + |00001111\rangle)$ and $|\beta\rangle = -1/\sqrt{2}(|11000011\rangle + |00111100\rangle)$. Thus, using the same code and universal fault-tolerant operations, we can prepare a generalized stabilizer state, $|\psi\rangle = a|\alpha\rangle + b|\beta\rangle$, where a, b are real numbers and $a^2 + b^2 = 1$.

2. BH_3 molecule

The logical states, $|\bar{\pm}\rangle$, of code in Sec. VC-3., are

$$\begin{aligned} |\alpha\rangle = & 1/\sqrt{2}(|11111000000\rangle + |110000111100\rangle + |110100111000\rangle + |111011000100\rangle), \text{ and} \\ |\beta\rangle = & -1/\sqrt{2}(|111000110100\rangle + |110100111000\rangle + |111100110000\rangle + |110111001000\rangle). \end{aligned}$$

Thus, using the same code and universal fault-tolerant operations, we can prepare a generalized stabilizer state, $|\psi\rangle = a|\alpha\rangle + b|\beta\rangle$, where a, b are real numbers and $a^2 + b^2 = 1$.

E. Circuit for preparing the generalized stabilizer states

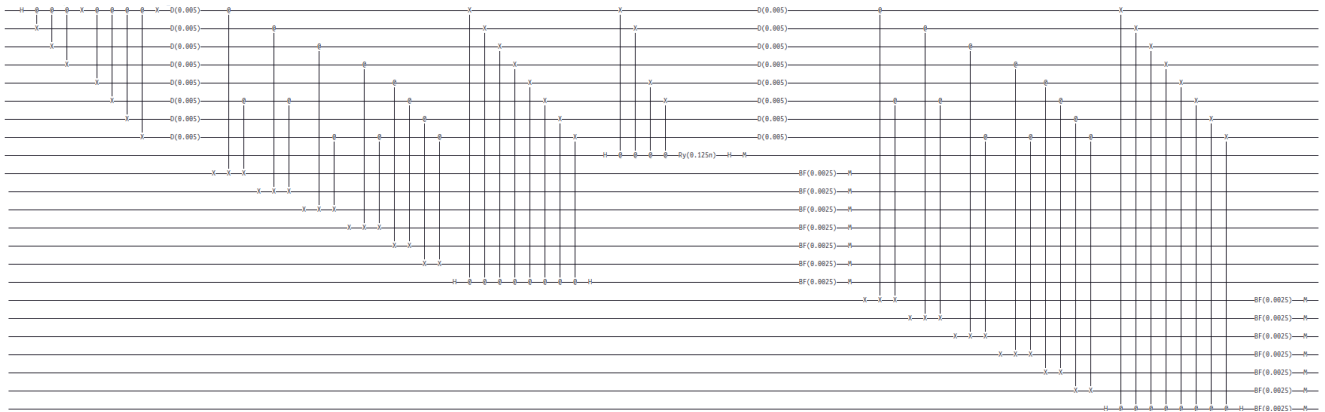


Figure 7. The circuit used for noisy preparation of a generalized stabilizer state for the case of H_4 molecule.